Lawrence Berkeley National Laboratory
Recent Work

Title

A flavin-based extracellular electron transfer mechanism in diverse Gram-positive bacteria.

Permalink

Journal

Nature, 562(7725)

ISSN

0028-0836

Authors

Light, Samuel H
Su, Lin
Rivera-Lugo, Rafael
et al.

Publication Date

2018-10-01

DOI

10.1038/s41586-018-0498-z

Peer reviewed

A flavin-based extracellular electron transfer mechanism in diverse gram-positive bacteria

Samuel H. Light[1], **Lin Su**[2,3], **Rafael Rivera-Lugo**[1], **Jose A. Cornejo**[2], **Alexander Louie**[1], **Anthony T. Iavarone**[4], **Caroline M. Ajo-Franklin**[2], and **Daniel A. Portnoy**[1,5]

[1]Department of Molecular and Cell Biology, University of California, Berkeley, Berkeley, CA, 94720

[2]Molecular Foundry, Molecular Biophysics and Integrated Biosciences, and Synthetic Biology Institute, Lawrence Berkeley National Laboratory, Berkeley, CA, 94720

[3]State Key Laboratory of Bioelectronics, Southeast University, Nanjing, 210018, China

[4]QB3/Chemistry Mass Spectrometry Facility, B207 Stanley Hall, University of California, Berkeley, Berkeley, CA, 94720

[5]School of Public Health, University of California, Berkeley, Berkeley, CA, 94720

Abstract

Extracellular electron transfer (EET) describes microbial bioelectrochemical processes in which electrons are transferred from the cytosol to the exterior of the cell.[1] Mineral-respiring bacteria employ elaborate heme-based electron transfer mechanisms,[2–4] but the existence or basis of other EETs remains largely unknown. In this study, we show that the foodborne pathogen *Listeria monocytogenes* utilizes a distinctive flavin-based EET mechanism to deliver electrons to iron or an electrode. A forward genetic screen to identify *L. monocytogenes* mutants with diminished extracellular ferric iron reductase activity led to the characterization of an 8-gene locus responsible for EET. This locus encodes a specialized NADH dehydrogenase that segregates EET from aerobic respiration by channeling electrons to a discrete membrane-localized quinone pool. Other proteins facilitate the assembly of an abundant extracellular flavoprotein that, in conjunction with free-molecule flavin shuttles, mediates electron transfer to extracellular acceptors. This system thus establishes a simple electron conduit compatible with the single-membrane gram-positive cell structure. Activation of EET supports growth on non-fermentable carbon sources and a EET mutant exhibited a competitive defect within the mouse gastrointestinal tract. Orthologs of the identified EET genes are present in hundreds of species across the Firmicutes phylum, including multiple pathogens and commensal members of the intestinal microbiota, and correlate with EET

activity in assayed strains. These findings suggest a surprising prevalence of EET-based growth capabilities and establish new relevance for electrogenic bacteria across diverse environments, including host-associated microbial communities and infectious disease.

Listeria monocytogenes is a fermentative gram-positive bacterium that is frequently associated with decaying plant matter in the environment, but which transforms into an intracellular pathogen upon encountering a mammalian host.[5] Despite lacking a lifecycle or genes conventionally associated with EET, a 25-year-old observation of extracellular ferric iron reductase activity[6] led us to question whether *L. monocytogenes* possessed a novel EET mechanism. Since electrons transferred out of the cell can be captured by an electrode, electrochemical measurements provide a useful tool for assaying EET.[7] Chronoamperometry experiments showing that *L. monocytogenes* produces a robust electric current in the presence of growth substrate thus provided evidence of EET (Fig. 1a, Extended Data Fig. 1a). Moreover, cyclic voltammetry experiments, which monitor electric current while the electrochemical potential is systematically varied, revealed a distinctive catalytic wave reminiscent of other electrochemically active bacteria (Extended Data Fig. 1b).[8,9]

To address the genetic basis of EET activity, ~50,000 colonies of a pooled *L. monocytogenes himar1* transposon library were grown on Fe^{3+}-containing agar plates. Mutants with decreased colorimetric change following an Fe^{2+}-indicator overlay were visually identified and the location of their transposon insertion was mapped to the genome (Fig. 1b). From this screen, thirty-four independent transposon insertions that localized to a largely uncharacterized 8.5-kilobase locus were identified – with at least one insertion disrupting each of the 8 genes in this region (Fig. 1c). Based on the putative function of protein products, genes in the EET locus were assigned names (*dmk-*, *eet-*, and *fmn-* prefixes) that are used hereafter. The only transposon insertions outside the identified locus disrupt *ribU*, the substrate-binding subunit of a riboflavin transporter (Fig. 1c).[10] After confirming that the mutants had diminished ferric iron reductase (Fig. 1d) and electrochemical activity (Fig. 1e, Extended Data Fig. 1b), we turned to the molecular basis of EET.

Type II NADH dehydrogenase, or Ndh1 in *L. monocytogenes*, catalyzes electron exchange from cytosolic NADH to a lipid-soluble quinone derivative, the first step in the respiratory electron transport chain.[11] One of the genes in the EET locus, *ndh2*, encodes a protein with an N-terminal type II NADH dehydrogenase domain and a unique transmembrane C-terminal domain that is absent from functionally characterized enzymes (Fig. 2a). Consistent with *ndh2* encoding a novel NADH dehydrogenase, we observed that EET activation correlated with cellular NAD+ levels (Extended Data Fig. 2). Furthermore, proteins encoded by two other genes in the EET locus, DmkA and DmkB, are homologous to enzymes MenA and HepT, which catalyze terminal steps in the production of the quinone demethylmenaquinone (Fig. 2b). In *E. coli*, the different quinones demethylmenaquinone, menaquinone, and ubiquinone are employed to selectively channel electrons to different electron acceptors.[12] By analogy, we reasoned that a distinct quinone derivative and NADH dehydrogenase might functionally segregate electron fluxes for EET and aerobic respiration.

To clarify the relationship between EET and aerobic respiration, we formulated an "aerobic respiration medium" that contained non-fermentable glycerol as the sole carbon source. Despite exhibiting wildtype levels of ferric iron reductase activity (Extended Data Fig. 3a), a positive control that lacked terminal cytochrome oxidases (Δ*cydAB*/Δ*qoxA*), Δ*menA*, *hepT*::tn, and Δ*ndh1* strains failed to grow on aerobic respiration medium (Fig. 2c). By contrast, EET mutants grew similarly to wildtype under these conditions (Fig. 2c). Moreover, *menG*, which encodes the enzyme that converts demethylmenaquinone to menaquinone, is contained on an operon with *hepT* and is essential for growth on aerobic respiration medium, but not ferric iron reductase activity (Fig. 2c, Extended Data Fig. 3). Collectively, these results support the conclusion that a demethylmenaquinone derivative used by Ndh2 and a menaquinone derivative used by Ndh1 are selective for downstream enzymes that function in EET and aerobic respiration, respectively (Fig. 2d).

We next sought to address downstream steps responsible for electron transfer from the quinone pool to extracellular electron acceptors. FmnB is a predicted lipoprotein that is annotated as possessing flavin mononucleotide (FMN) transferase activity. Homologous FMN transferases catalyze a posttranslational modification in which an FMN moiety is covalently linked to a threonine sidechain of substrate proteins (Fig. 3a).[13,14] To identify protein substrates of FmnB, wildtype and *fmnB*::tn cells were subjected to a comparative mass spectrometric analysis. Only two *L. monocytogenes* peptides met the criteria of selective FMNylation in the wildtype sample and both of these mapped to distinct regions in the protein product of the neighboring gene in the EET locus, PplA (Supplementary Table 1).

Like FmnB, PplA is a predicted lipoprotein and a trypsin-shaving experimental approach, in which extracellular surface-associated proteins liberated through a partial digestion of the cell wall are identified by mass spectrometry, confirmed that PplA is associated with the surface of the cell (Supplementary Table 2). The N-terminal lipidation site on PplA is followed by ~30 amino acids that are predicted to be unstructured. N-terminal unstructured regions are a common feature of bacterial lipoproteins and are thought to provide a loose tether that allows the active portion of the protein to diffuse further from the membrane and to partially or fully penetrate the cell wall.[15] Thus, this property coupled with the covalently bound redox-active FMNs is consistent with PplA representing the extracellular component of the EET machinery that facilitates electron transfer, via its FMNs, to extracellular electron acceptors.

Following its unstructured N-terminal region, PplA has sequential domains that share 59% sequence identity with each other. From the proteomic analysis, it is evident that the FMNylated threonines on PplA assume equivalent positions on each of these related domains (Fig. 3b). To further clarify the mechanism of FMNylation, FmnB substrate specificity was tested using recombinant FmnB and PplA. These assays confirm that FmnB catalyzes FMNylation of PplA and demonstrate that the enzyme specifically uses flavin adenine dinucleotide (FAD) as substrate (Fig. 3c, Extended Data Fig. 4).

Considering that both FmnB and PplA are membrane-anchored lipoproteins, FmnB must require a mechanism of acquiring FAD substrate in order to modify PplA. The only

transposon insertions identified outside the EET locus disrupt *ribU*, which has previously been shown to encode the substrate-binding subunit of an ECF (energy-coupling factor) transporter that functions in riboflavin uptake.[10] In addition to a substrate-binding subunit, ECF transporters contain a transmembrane subunit and two distinct ATPase subunits, which drive transport of substrate across the membrane (Extended Data Fig. 5a).[10] FmnA in the EET locus shares 50% sequence identity with EcfT, the transmembrane subunit of the RibU-ECF riboflavin transporter, and this led us to hypothesize that it might interact with RibU to promote FAD secretion (Extended Data Fig. 5b). Consistent with this interpretation, proteomic analysis of *ribU*::tn and *fmnA*::tn strains revealed a dramatic decrease in PplA FMNylation (Supplementary Table 1). Furthermore, addition of FAD to the growth medium specifically restored ferric iron reductase activity to the *ribU*::tn and *fmnA*::tn strains (Extended Data Fig. 5c). Based on these findings, we propose that RibU and FmnA establish a transporter that secretes the FAD required for FmnB-catalyzed FMNylation of PplA.

The term "extracellular electron shuttle" refers to redox-active small molecules that are cyclically reduced by cells and oxidized by extracellular electron acceptors.[16,17] The relevance of shuttles for EET is exemplified by *Shewanella* species, which use an efflux-type transporter to secrete flavins that can shuttle electrons to acceptors that are not directly contacting the cell.[18–20] In contrast to *Shewanella*, *L. monocytogenes* is a flavin auxotroph and thus, by definition, environmental flavins *must* be present in its replicative niche. Indeed, micromolar flavin concentrations are typical of nutrient-rich environments, like the plant/animal biomass and mammalian host where *L. monocytogenes* proliferates.[21,22] To determine whether flavins could be used as electron shuttles, we tested the effect of exogenous riboflavin, FMN, and FAD on EET activity. Injection of FMN into an *L. monocytogenes*-inoculated electrochemical chamber resulted in a pronounced increase in electric current (Extended Data Fig. 6a). Moreover, while flavins caused a marked concentration-dependent enhancement in the reduction of insoluble ferric (hydr)oxide, cells immersed in soluble ferric iron exhibited a high baseline level of activity that was unresponsive to flavins (Extended Data Fig. 6b). These data thus support the conclusion that *L. monocytogenes* can use environmental flavins to shuttle electrons to outlying acceptors.

Integrating insight into the role of the components of the EET apparatus, we arrive at a molecular model of electron travel from intracellular NADH, to membrane-confined quinone, to extracellular flavoprotein/shuttles, and ultimately to a kinetically favorable terminal electron acceptor (Fig. 3d). Next, to determine whether EET established a *bona fide* growth-supporting activity, we screened a library of common microbial growth substrates and found that the inclusion of ferric iron or an electrode was required for anaerobic growth on the sugar alcohols xylitol and D-arabitol (Fig. 4a, Extended Data Fig. 7). Moreover, while genes for aerobic respiration, but not EET, were essential for aerobic growth on xylitol, this pattern was reversed under anaerobic conditions, with the EET genes being essential and aerobic respiration genes dispensable (Fig. 4a, Extended Data Fig. 7). These data thus demonstrate that the distinct electron transport chains that segregate aerobic respiration and EET promote aerobic and anaerobic growth, respectively.

We next asked whether EET played a role in host colonization. Consistent with EET being dispensable for aerobic growth, EET-deficient mutants resembled wildtype *L.*

monocytogenes in an intracellular macrophage growth assay and an intravenous infection model (Extended Data Fig. 8). Since anaerobic growth mechanisms are important for microbial proliferation within the intestinal lumen,[23,24] we hypothesized that the foodborne pathogen might utilize EET in this context. Consistent with the hypothesis, the fecal burden of the *ndh2*::tn strain was decreased ~6-fold in a streptomycin-pretreated model of *L. monocytogenes* intestinal colonization (Fig 4b). These results thus suggest a role for EET within the dysbiotic gut and raise the possibility that EET establishes a generally significant metabolic activity within the mammalian gastrointestinal tract.

We next turned to the phylogenetic distribution of the identified EET genes. BLAST searches revealed that homologs of the genes are widespread in hundreds of species that span the Firmicutes phylum (Extended Data Fig. 9a, Supplementary Table 3). Many of these genes likely encode functional EET systems, as the identified locus is typically conserved, though noteworthy distinctions are evident in some genomes (Extended Data Fig. 9b). Microbes that possess a locus with EET genes adopt a wide range of different lifestyles, including within thermophilic (*Caldanaerobius*, *Thermoanaerobacter*, etc.) and halophilic (*Halolactibacilli*, *Halothermothrix*, etc.) habitats. Orthologs of the identified EET genes are found in a number of human pathogens (*Clostridium perfringens, Enterococcus faecalis, Streptococcus dysgalactiae*, etc.), members of the human microbiota (*Clostridia, Enterococci, Streptococci*, etc.), and lactic acid bacteria that have commercial applications in food fermentation or probiotics (*Lactococci, Lactobacilli, Oenococci, Tetragenococci*, etc.) (Supplementary Table 3). Functionality of identified loci could explain previous reports of EET-like activity in a number of species[25–35] and assays of ferric iron reductase activity of a panel of Firmicutes provided additional evidence that the presence of necessary genetic components correlates with EET activity (Fig. 4c).

In conclusion, the studies presented here establish a novel electron transport chain that supports growth on extracellular electron acceptors. This mechanism lacks an elaborate multi-heme apparatus and, partly by taking advantage of the single-membrane gram-positive cell architecture, is characterized by significantly fewer electron transfer steps than comparable systems in mineral-respiring gram-negative bacteria.[1] Interestingly, the identified EET genes are present in a wide-ranging group of microorganisms that occupy a diverse array of ecological niches. Defying conventional views of EET, this distinctive system is abundant in bacteria that prioritize fermentative metabolic strategies and reside in nutrient-rich environments, including the lactic acid bacteria. Within this context, environmental flavins seems to represent a feature of the ecological landscape that can be exploited to promote EET activity. These observations suggest that, rather than a specialized process confined to mineral-respiring bacteria, utilization of extracellular electron acceptors represents a fundamental facet of microbial metabolism relevant across diverse environments. In addition to obvious bioenergetic applications, characterization of flavin-based EET mechanism thus establishes new avenues for the study of electrochemical activities throughout the microbial world.

Methods

L. monocytogenes strains and growth conditions.

All *L. monocytogenes* strains used in this study were derived from wildtype 10403S (Supplementary Table 4). Transduction methods were used to introduce transposons into distinct genetic backgrounds, as previously described.[37,38] *L. monocytogenes* cells were grown at 37 °C and spectrophotometrically measured by optical density at a wavelength of 600 nm (OD_{600}). Anaerobic conditions were achieved with the BD GasPak™ EZ pouch system or an anaerobic chamber (Coy Laboratory Products) with an environment of 2% H_2 balanced in N_2.

Filter-sterilized brain-heart infusion medium (Difco) or variants of chemically defined Listeria synthetic medium (LSM)[39] were used in all studies. "Aerobic respiration medium" replaced the glucose in LSM with 50 mM glycerol. The requirement of an electron acceptor to support *L. monocytogenes* growth on xylitol was identified by comparing aerobic versus anaerobic (absent an alternative electron acceptor) growth on carbon sources, using PM1 and PM2A plates of the Phenotype MicroArray (Biolog). "Xylitol medium" replaced the glucose in LSM with 50 mM xylitol.

Gene name assignment.

The identified EET locus is widely conserved in *L. monocytogenes* isolates and encompasses the genes *lmrg_02179-lmrg_02186* in *L. monocytogenes* 10403S (which correspond to *lmo2634-lmo2641* in *L. monocytogenes* EGD-e). Identified EET genes were assigned *dmk* or *fmn* prefixes based on putative roles in demethylmenaquinone biosynthesis or PplA FMNylation, respectively. The *eet* prefix was assigned to the remaining genes, which at present lack high-confidence functional assignments. The only previously named gene, *pplA*, was so called based on the role of its cleaved signal peptide as a signaling pheromone (a function that seems unrelated to the mature protein).[40]

Bioelectrochemical characterization and measurements.

Chronoamperometry and cyclic voltammetry were carried out using a Bio-Logic Science Instruments potentiostat model VSP-300. All measurements were performed using double chamber electrochemical cells (Extended Data Fig. 1a) and consisted of an Ag/AgCl reference electrode (CH Instruments), a Pt wire counter electrode (Alfa Aesar), and a 6.35 mm-thick graphite felt working electrode with a 16-mm radius (Alfa Aesar).

Electrochemical cells were prepared with 120 mL of modified LSM (containing 0.8 μM FMN as the sole flavin) and an open circuit potential was performed in the absence of bacteria. Once the current stabilized, the electrochemical cell was inoculated to a final OD_{600} of ~0.1. The medium in the electrochemical chamber was mixed with a magnetic stir bar for the course of the experiment. For current acquisition, the applied potential was set at +0.4 V vs Ag/AgCl. To maintain anaerobic conditions, electrochemical cells were continuously purged with N_2 gas. Cyclic voltammetry measurements in the potential region of −0.8 to +0.4 V vs Ag/AgCl and a scan rate of 10 mV s^{-1} were conducted immediately prior to inoculation and 3 hours later. Electric currents are reported as a function of the

geometric surface area of the electrode. To test the effect of flavins on electrochemical activity, FMN was injected into the *L. monocytogenes*-inoculated electrochemical chamber to a final concentration of 1 μM.

For *S. oneidensis* experiments, the glucose in LSM was replaced with sodium lactate and *S. oneidensis* was inoculated to an OD_{600} of 0.1. Growth-supporting *L. monocytogenes* experiments on xylitol medium were conducted in a similar fashion, but the electrochemical cell was inoculated to an OD_{600} of ~0.002 and the medium from the electrochemical chamber was sampled at regular intervals for the enumeration of CFU.

Screen of mutants with diminished ferric iron reductase activity.

A previously described method was adapted to screen for *L. monocytogenes* mutants with diminished ferric iron reductase activity.[6] Approximately 250 colony-forming units/plate of a pooled *himar1* transposon library, generated as previously described,[38] were grown on brain-heart infusion agar supplemented with 0.1 mg/mL ferric ammonium citrate. After 24 hours at 37 °C, plates were removed from the incubator and a 10-mL overlay (0.8% agarose and 2 mM ferrozine) was applied. Colorimetric change resulting from ferrozine binding to Fe^{2+} was visually tracked for ~10 minutes. Colonies with diminished colorimetric change were selected and the location of the transposon insertion identified by Sanger sequencing, as previously described.[41]

Ferrozine assay of ferric iron reductase activity.

L. monocytogenes cells grown to mid-log phase were washed twice, normalized to an OD_{600} of 0.5, and resuspended in fresh medium supplemented with 4 mM ferrozine. Experiments were initiated by adding 100 μL of cells to an equivalent volume of 50 mM ferric ammonium citrate or ferric (hydr)oxide and were conducted in triplicate at 37 °C in 96-well format using a plate reader. OD_{562} measurements were made every 30 seconds for up to an hour. Maximal rates (typically over 2 minutes) calculated from a Fe^{2+} standard curve are reported. Assays were generally performed in LSM, with glucose serving as the electron donor. However, because some of the respiratory mutants grew poorly in these conditions, these strains were assayed in brain-heart infusion medium (with glucose remaining as the electron donor). For FAD complementation studies, prior to washing steps, strains grown to mid-log were split and, after adding 0.5 mM FAD to one aliquot, incubated for 1 hour at 37 °C. To test the effect of flavins, riboflavin, FMN, or FAD was titrated into cells resuspended in a LSM base that lacked flavins.

To prepare other species (detailed in Supplementary Table 4) for the ferric iron reductase assay, cells were grown anaerobically in brain-heart infusion medium for 36 hours. Sub-cultures in brain-heart infusion medium supplemented with 25 mM ferric ammonium citrate were then grown to mid-log phase. Cells were washed twice, resuspended in fresh brain-heart infusion medium, and cell densities were normalized to wildtype *L. monocytogenes*. Next, ferrozine was added to a final concentration of 2 mM and 100 μL of cells were dispensed in a 96-well plate. The experiment was initiated by adding 100 μL of brain-heart infusion medium supplemented with 10 mM ferric ammonium citrate and OD_{562} measurements were made as described for the *L. monocytogenes* ferric iron reductase assay.

L. monocytogenes growth on xylitol and ferric iron.

To test electron acceptor usage capabilities, xylitol medium was inoculated with *L. monocytogenes* and incubated at 25° C in an anaerobic chamber. Conditions testing putative electron acceptors contained 50 mM ferric ammonium citrate or ferric (hydr)oxide, prepared as previously described.[42] For the ferric ammonium citrate experiments, 50 mM sodium citrate was included in the ferric ammonium citrate-lacking control condition and CFU were enumerated following overnight incubation in a 96-well plate (Greiner Bio-One). Ferric (hydr)oxide experiments were conducted in 6-well plate (Costar) and CFU were enumerated 6 days after inoculation.

NAD+/NADH measurements.

L. monocytogenes cells grown overnight in LSM were washed and resuspended in 500 μL of medium. Cells were then split and 50 mM ferric ammonium citrate was added to one aliquot. To test aerobic conditions, 14-mL tubes were placed in a shaking (200 RPM) incubator. To achieve microaerophilic conditions, the headspace in the tube was purged with argon gas and the tightly capped tube was placed in a stationary incubator. After 1.5 hours at 37°C, bacteria were harvested by centrifugation, resuspended in PBS, and lysed by vortexing with 0.1 mm-diameter zirconia-silica beads. NAD+/NADH measurements were performed using the NAD/NADH-Glo Assay (Promega).

Assay of FmnB FMN transferase activity

Constructs of *fmnB* and *pplA* that truncated the signal peptide were subcloned into the pMCSG58 vector. Protein overexpression and purification followed previously described protocols.[43] Purified PplA and FmnB were incubated overnight at a 10:1 molar ratio in assay buffer (0.5 M NaCl and 10 mM Tris, pH 8.3) with putative flavins substrates. Since homologous FMN transferases require a magnesium cofactor,[13] the effect of the chelator ethylenediaminetetraacetic acid (EDTA) on activity was tested. Samples were analyzed by SDS-PAGE and protein bands with covalent flavin modifications were visualized by UV illumination.

To identify the basis of posttranslational modifications, intact protein mass measurements of PplA were made using a Synapt G2-S*i* mass spectrometer that was equipped with an electrospray ionization (ESI) source and a C_4 protein ionKey (inner diameter: 150 μm, length: 50 mm, particle size: 1.7 μm), and connected in-line with an Acquity M-class ultra-performance liquid chromatography system (UPLC; Waters, Milford, MA). Acetonitrile, formic acid (Fisher Optima grade, 99.9%), and water purified to a resistivity of 18.2 MΩ·cm (at 25 °C) using a Milli-Q Gradient ultrapure water purification system (Millipore, Billerica, MA) were used to prepare mobile phase solvents. Solvent A was 99.9% water/0.1% formic acid and solvent B was 99.9% acetonitrile/0.1% formic acid (v/v). The elution program consisted of a linear gradient from 1% to 10% B (v/v) over 1 min, a linear gradient from 10% to 90% B over 4 min, isocratic flow at 90% B for 5 min, a linear gradient from 90% to 1% B over 2 min, and isocratic flow at 1% B for 18 min, at a flow rate of 2 μL/min. The ionKey column and the autosampler compartment were maintained at 40 °C and 6 °C, respectively. Mass spectra were acquired in the positive ion mode and continuum format, operating the time-of-flight (TOF) analyzer in resolution mode, with a scan time of 0.5 s,

over the range m/z = 400 to 5000. Mass spectral deconvolution was performed using ProMass software (version 2.5 SR-1, Novatia, Monmouth Junction, NJ).

L. monocytogenes protein trypsinization.

One milliliter of *L. monocytogenes* cells grown in LSM to mid-log phase was washed, resuspended in 100 μL of 100 mM NH_4HCO_3 (pH 7.5), and incubated at 100 °C for 10 minutes. Cells were lysed by bead beating for 15 minutes at 4 °C. RapiGest SF (Waters) was added to lysed cells at a final concentration of 0.1% and the sample was incubated at 100 °C for 5 minutes. After adding 5 μL of 100 mM dithiothreitol, samples were incubated at 58 °C for 30 minutes. Next, 15 μL of 100 mM iodoacetamide was added and sample were incubated for an additional 30 minutes. Samples were then digested overnight with 10 μL Trypsin Gold (Promega). The following morning, 10 μL of 5% trifluoroacetic acid was added and samples were incubated at 37 °C for 90 minutes. Samples were centrifuged for 30 minutes, to remove hydrolyzed RapiGest, and supernatant was collected.

L. monocytogenes intracellular growth assays.

Bone marrow-derived macrophages prepared from 6- to 8-week-old female mice were plated overnight on coverslips and infected with *L. monocytogenes* strains at a multiplicity of infection of 0.1. Macrophage monolayers were washed with PBS and fresh medium was added thirty minutes after infection. At 1 hour post-infection, 50 μg/mL gentamicin was added to kill extracellular bacteria. To enumerate *L. monocytogenes* CFU, macrophages were lysed by transferring coverslips to 10 mL of water, as previously described.[44]

L. monocytogenes intravenous infections.

Eight-week-old female C57BL/6 mice (The Jackson Laboratory) were infected with 1×10^5 CFU in 200 μL of PBS by tail vein injection. Forty-eight hours post-infection, spleens and livers were harvested, homogenized, and plated for the enumeration of CFU.

L. monocytogenes oral infections.

Previously described models of *L. monocytogenes* oral infection were adapted to address the role of EET in the intestinal lumen.[45,46] Prior to infection, 5 mg/mL of streptomycin sulfate was added to the drinking water of 8-week-old female C57BL/6 mice (The Jackson Laboratory). After 24 hours, mice were transferred to fresh cages and chow was removed to initiate an overnight fast. Forty-eight hours after streptomycin addition to the water, mice were isolated, fed a small piece of bread with 3 μL of butter and an inoculum with 10^8 CFU of *L. monocytogenes*, and returned to cages containing standard drinking water and chow. To confine *L. monocytogenes* to the intestinal lumen, a Δ*hly* parental strain (which have greatly reduced intracellular growth and spread) was used in these experiments. Inoculums were prepared with a 1:1 ratio of Δ*hly* and an erythromycin-resistant Δ*hly* strain (Δ*hly*/*erm*[R], derived as previously described[47]) or Δ*hly* and Δ*hly*/*ndh2*::tn. Following infection, stools were collected, homogenized, and dilutions were plated. Because total parental strain CFU did not statistically differ between conditions, results are simply reported as a competitive index (i.e., the ratio of streptomycin to erythromycin-resistant CFU). This study was carried out in strict accordance with the recommendations in the Guide for the Care and Use of

Laboratory Animals of the National Institutes of Health. All protocols were reviewed and approved by the Animal Care and Use Committee at the University of California, Berkeley (AUP-2016–05-8811).

Identification of protein substrates of FmnB.

Wildtype and *fmnB*::tn strains grown in LSM were prepared for proteomic analysis as described in the protein trypsinization section. Peptides with >50% FMNylated peptide relative ion abundance in the wildtype sample and <5% in the *fmnB*::tn sample were identified using Progenesis QI for Proteomics software (version 4.0, Waters) and validated by manual inspection of the data. To address the FMNylation status of PplA, *ribU::tn* and *fmnA*::tn mutants were prepared in the same manner.

Trypsin-shaving analysis of surface-associated proteins.

Trypsin-shaving experiments adapted a previously described method.[4] Cells grown in brain-heart infusion medium were washed twice and resuspended in a shaving buffer (1 M sucrose + 1 mM HEPES, pH 7). Lysozyme from chicken egg white (Sigma) was added to a concentration of 0.1 mg/mL. Cells were incubated at 37 °C for 60 minutes and released surface-associated components were separated from the cell by centrifugation. The supernatant (surface-associated protein fraction) was dialyzed overnight in digestion buffer (100 mM NH_4HCO_3, pH 7.5) and the pellet (total protein fraction) was resuspended in digestion buffer. Samples were prepared for proteomic experiments as described in the protein trypsinization section. A label-free relative quantification approach[48,49] implemented in Progenesis QI for Proteomics software (version 4.0, Waters) identified proteins disproportionately abundant in the surface-associated fraction.

Liquid chromatography-mass spectrometry analysis of trypsin-digested proteins.

Samples of trypsin-digested proteins were analyzed in triplicate using the Acquity M-class UPLC and Synapt G2-S*i* mass spectrometer, as follows. The mass spectrometer was equipped with a nanoelectrospray ionization (nanoESI) source that was connected in-line with the UPLC. The UPLC was equipped with trapping (Symmetry C18, inner diameter: 180 μm, length: 20 mm, particle size: 5 μm) and analytical (HSS T3, inner diameter: 75 μm, length: 250 mm, particle size: 1.8 μm, Waters) columns. Solvent A was 99.9% water/0.1% formic acid and solvent B was 99.9% acetonitrile/0.1% formic acid (v/v). The elution program consisted of a linear gradient from 1% to 10% B (v/v) over 2 min, a linear gradient from 10% to 35% B over 90 min, a linear gradient from 35% to 90% B over 1 min, isocratic flow at 90% B for 6 min, a linear gradient from 90% to 1% B over 1 min, and isocratic flow at 1% B for 20 min, at a flow rate of 300 nL/min. The column and autosampler compartments were maintained at 35 °C and 6 °C, respectively. Ion mobility-enabled HD-MS^E data[50,51] were acquired in the positive ion mode and continuum format, operating the TOF analyzer in resolution mode, with a scan time of 0.5 s, over the range m/z = 50 to 2000. An optimized wave velocity of 850 m/s was used for the traveling wave ion mobility cell. Collision-induced dissociation was performed in the ion transfer cell with a collision energy ramp from 30 to 78 V. Data acquisition was controlled using MassLynx software (version 4.1), and tryptic peptides were identified using Progenesis QI for Proteomics software (version 4.0, Waters).

Bioinformatics analysis of identified EET genes.

Ndh2 homologs were identified by searching the sequence of the unique C-terminal domain of Ndh2 on the PSI-BLAST server.[52] To perform a phylogenetic analysis, representative homologs were selected and aligned by ClustalW.[53] The maximum likelihood method was used to infer the evolutionary history of identified sequences in Mega 7.0.26 and confidence limits of branch points were estimated by 1,000 bootstrap replications.[54,55] The information about EET genetic loci summarized in Supplementary Table 3 was acquired by analyzing genomic context of identified genes in the PATRIC 3.5.1 (https://www.patricbrc.org) database.

Statistics and reproducibility.

No statistical methods were used to pre-determine sample size. The investigators were not blinded to allocation during experiments and outcome assessment. Statistical analyses were performed in Prism 5 for Mac OS X (GraphPad Software) and Progenesis QI for Proteomics version 4.0.

Data availability statement.

The datasets generated during the current study are available from the corresponding author on reasonable request.
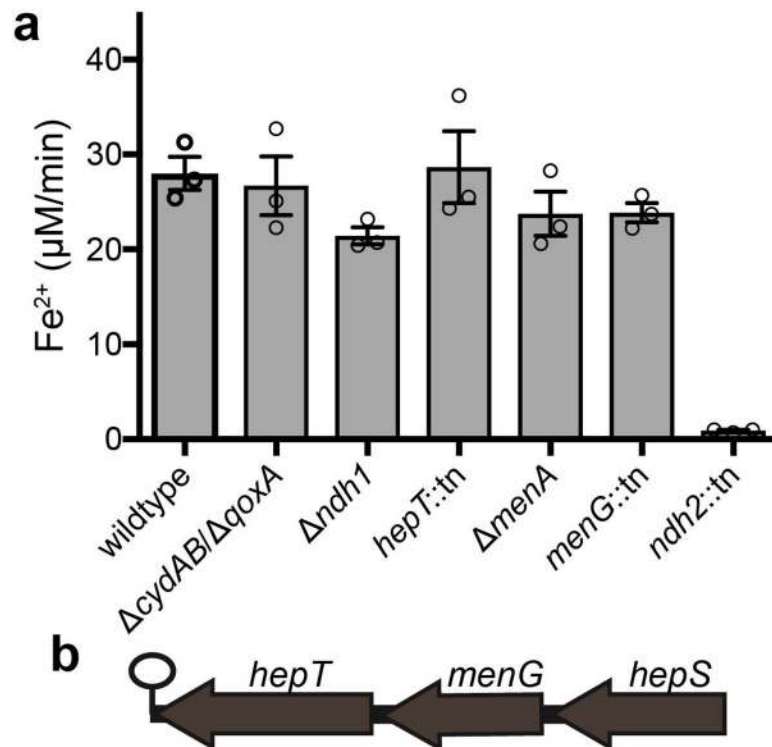
Extended Data
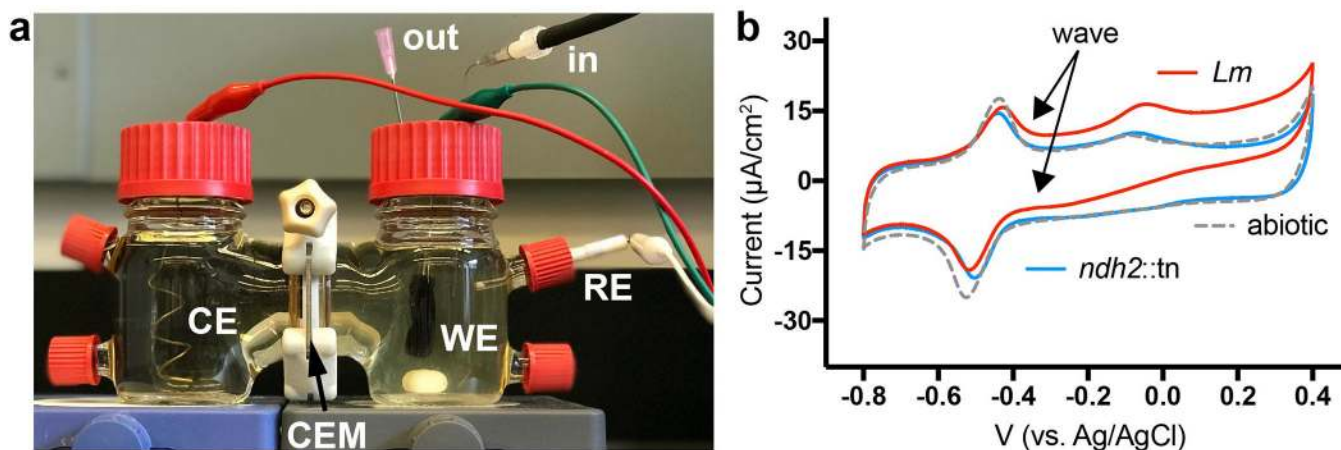
Extended Data Figure 1. Electrochemical analyses of *L. monocytogenes*.
(a) The double chamber cell used for electrochemical experiments. Abbreviations stand for: working electrode (WE), reference electrode (RE), counter electrode (CE), cation exchange membrane (CEM). Inlets and outlets for N_2 gas are labeled. (b) Cyclic voltammograms of wildtype and *ndh2*::tn *L. monocytogenes* strains. "Abiotic" refers to an uninoculated control. Arrows highlight the initiation of the catalytic wave. Results are representative of three independent experiments ($n = 3$).
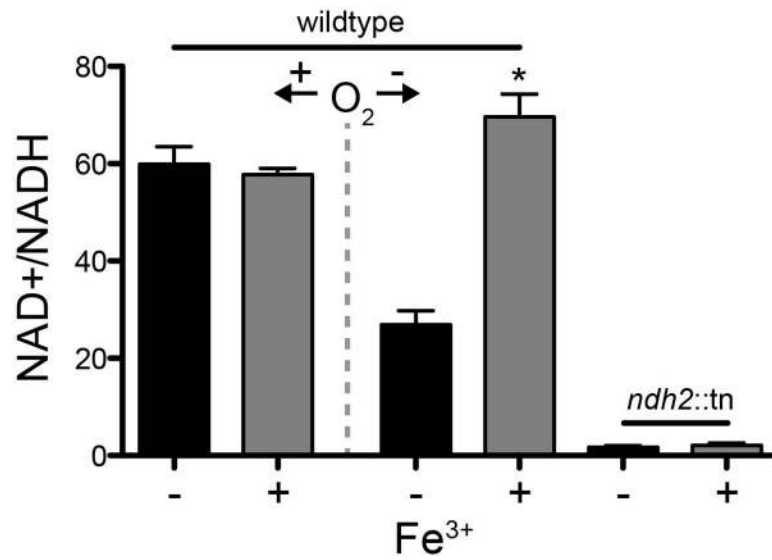
Extended Data Figure 2. EET activity maintains cellular redox homeostasis.
NAD+/NADH ratio in wildtype and *ndh2*::tn strains supplemented with ferric ammonium citrate under aerobic or microaerophilic conditions. Results from three independent experiments ($n = 3$) are expressed as means and standard errors. A statistically significant difference (*, $P = 0.0015$ [unpaired two-sided *t* test]) between microaerophilic cells incubated with or without iron is indicated.


Extended Data Figure 3. Evidence that a distinct menaquinone derivative functions in aerobic respiration.

(a) Ferric iron reductase activity of mutants described in Fig. 2 demonstrates that genes essential for growth on aerobic respiration media are dispensable for EET. Results from three independent experiments ($n = 3$) are expressed as means and standard errors. (b) The *L. monocytogenes hep/men* operon. Notably, the demethylmenaquinone transferase, *menG*, which encodes the enzyme that converts demethylmenaquinone to menaquione (Fig. 2b), neighbors the *hepT* and *hepS* genes, which function in quinone biosynthesis and are essential for aerobic respiration (Fig. 2c).
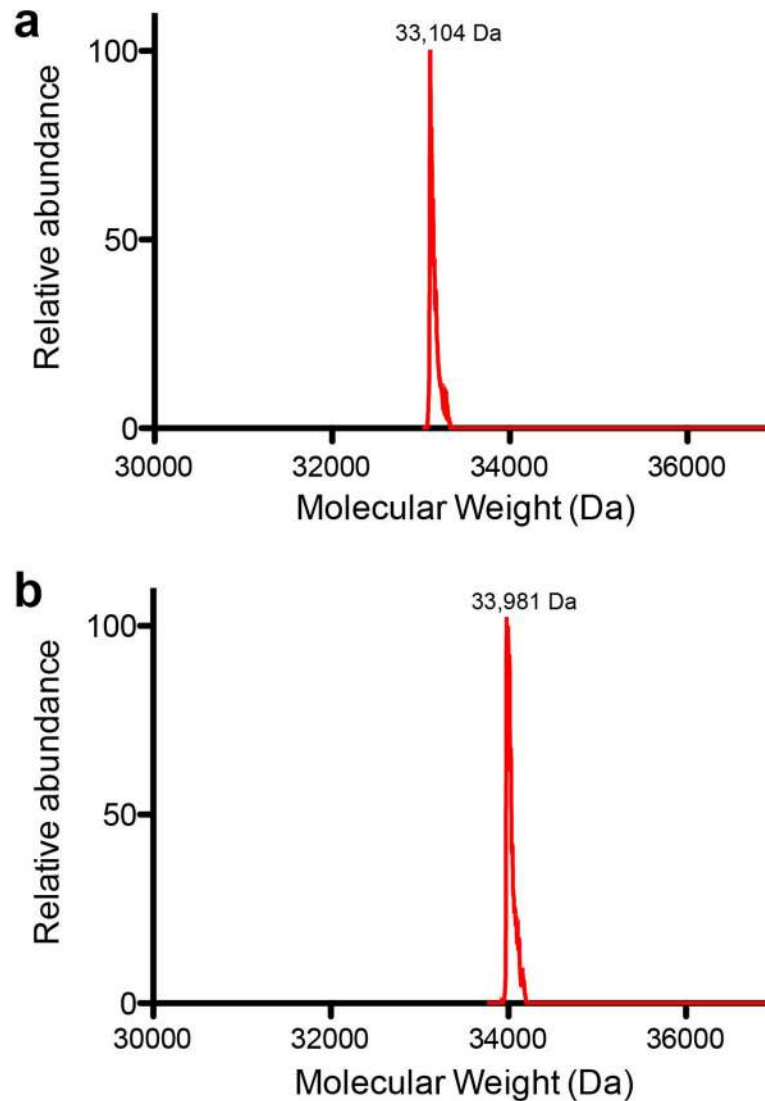
Extended Data Figure 4. Recombinant FmnB FMNylates PplA at two discrete sites.
Deconvoluted mass spectra from a single experiment ($n = 1$) of (a) recombinant PplA and (b) recombinant PplA incubated with FAD + FmnB. The observed molecular weight change (877 Da) is consistent with two posttranslational FMNylations (2×438.3 Da) on PplA.
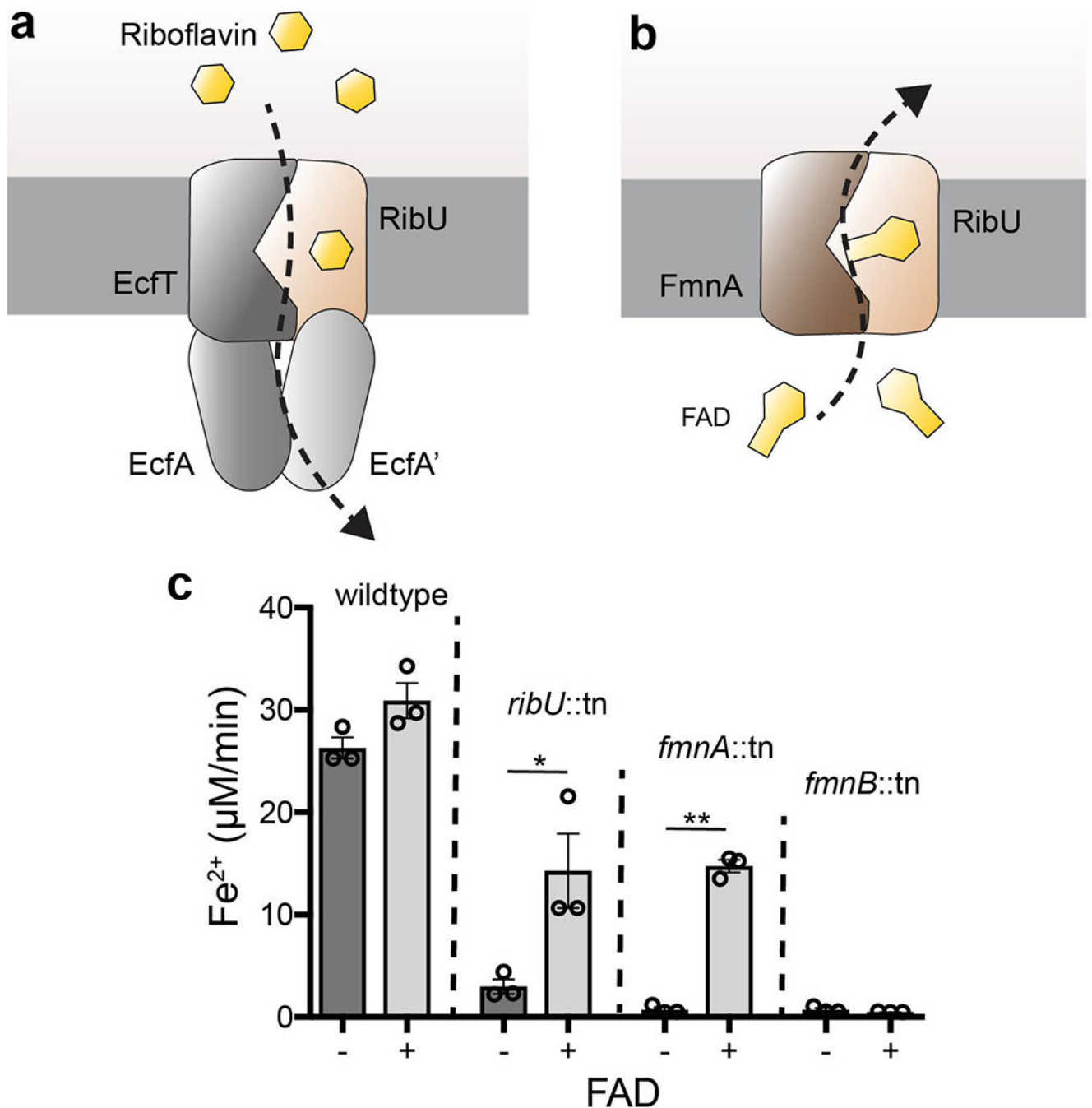
**Extended Data Figure 5. Proposed role of RibU and FmnA in FAD secretion.**
(a) Simplified adaptation of a previously proposed model of *L. monocytogenes* riboflavin uptake through the RibU, EcfT, EcfA, and EcfA' transporter.[10] According to this model, EcfT, EcfA, and EcfA' couple ATP hydrolysis with conformational changes that result in substrate bound to RibU being released into the cytosol. (b) Based on protein homology (FmnA shares 50% sequence identity with EcfT) and the expectation that extracellular FAD is required for FmnB to catalyze FMNylation of PplA, we propose the FmnA interacts with RibU to promote FAD secretion. (c) Ferric iron reductase activity of strains incubated with

0.5 mM FAD for 1 hour. The ability of exogenous FAD to specifically rescue ferric iron reductase activity to the *fmnA*::tn and *ribU*::tn strains is consistent with FmnA and RibU functioning in FAD secretion. Results from three independent experiments ($n = 3$) are expressed as means and standard errors. Statistically significant differences (*, $P = 0.038$ and **, $P < 0.0001$ [unpaired two-sided t test]) between untreated and FAD-treated cells are indicated.
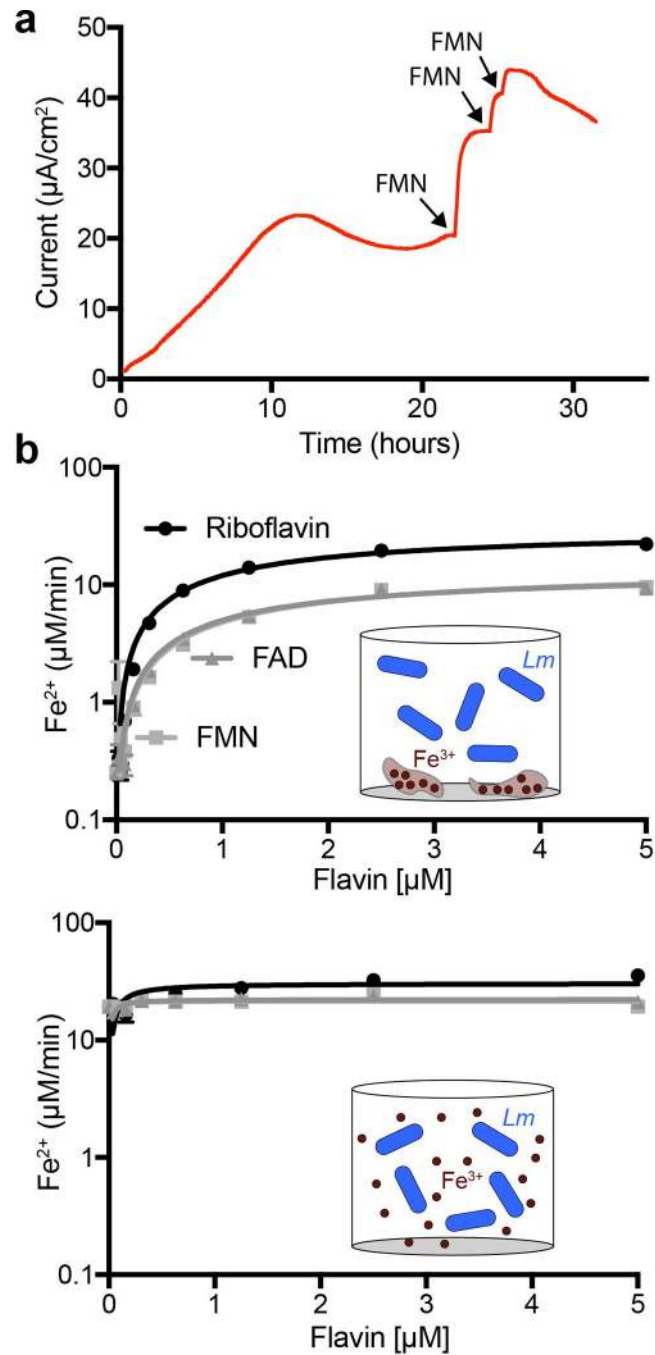
**Extended Data Figure 6. Flavin shuttles promote EET activity.**

(a) Chronoamperometry results from *L. monocytogenes*-inoculated electrochemical reactors with 1 μM FMN injections at the indicated time points. Results are representative of three independent experiments ($n = 3$). (b) The effect of flavins on *L. monocytogenes* (*Lm*) ferric iron reductase activity with insoluble ferric (hydr)oxide (top) and soluble ferric ammonium citrate (bottom). With insoluble substrate the local iron concentration for most cells is low, whereas with soluble substrate the concentration of iron in the direct vicinity of cells is high (insets). Results from three independent experiments ($n = 3$) are expressed as means and standard errors.
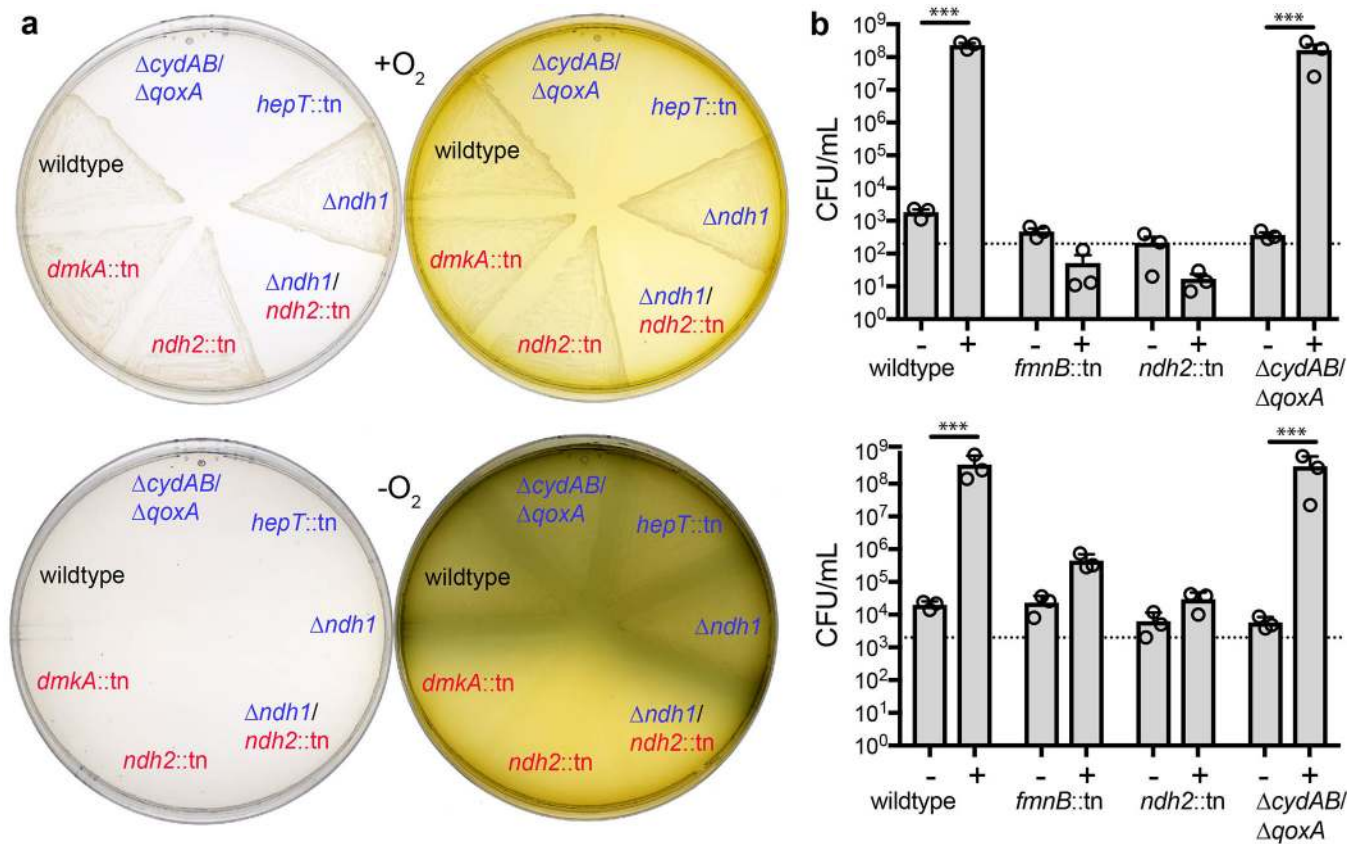
Extended Data Figure 7. EET supports anaerobic growth on ferric iron.

(a) Growth following incubation of *L. monocytogenes* strains on xylitol media without (left) or with (right) ferric iron under aerobic (top) or anaerobic (bottom) conditions. Results are representative of three independent experiments ($n = 3$). Strain labels are colored based on attributed deficiencies (Fig. 2d) in aerobic respiration (blue) or EET (red). Ndh1 and Ndh2 are likely functionally redundant under aerobic conditions, as a growth phenotype is only observed in the double mutant. Note that visual evidence of ferrous iron production in the agar adjoining anaerobically growing cells. (b) CFU of *L. monocytogenes* strains anaerobically incubated in xylitol media without (−) or with (+) ferric supplementation. Results for soluble ferric ammonium citrate (top) and insoluble ferric (hydr)oxide (bottom) are shown. Dashed lines denote the number of cells at the start of the of the experiment. Results from three independent experiments ($n = 3$) are expressed as means and standard

errors. Statistically significant differences (***, $P < 0.0001$ [unpaired two-sided t test]) in the ferric iron-supplemented condition are noted.
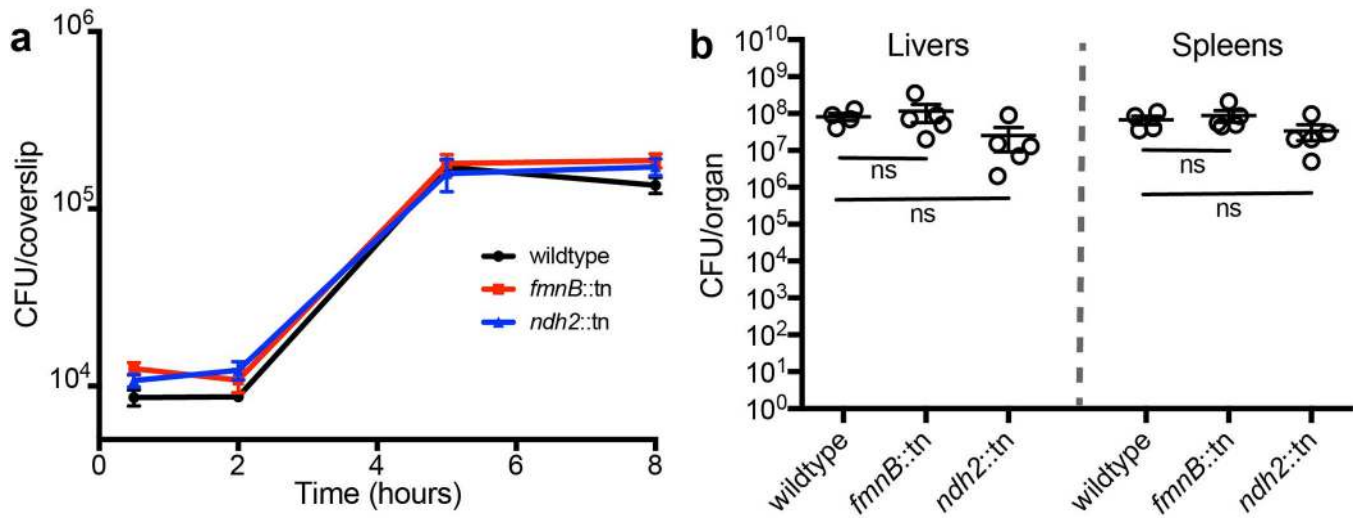
Extended Data Figure 8. EET genes are dispensable for *L. monocytogenes* intracellular growth.
(a) Murine bone-marrow-derived macrophages were infected with *L. monocytogenes* and CFU were enumerated at the indicated times. Results from three independent experiments ($n = 3$) are expressed as means and standard errors. (b) *L. monocytogenes* burdens in mouse organs 48 hours after intravenous infection. Representative results from two independent experiments ($n = 2$) are expressed as medians and standard errors.
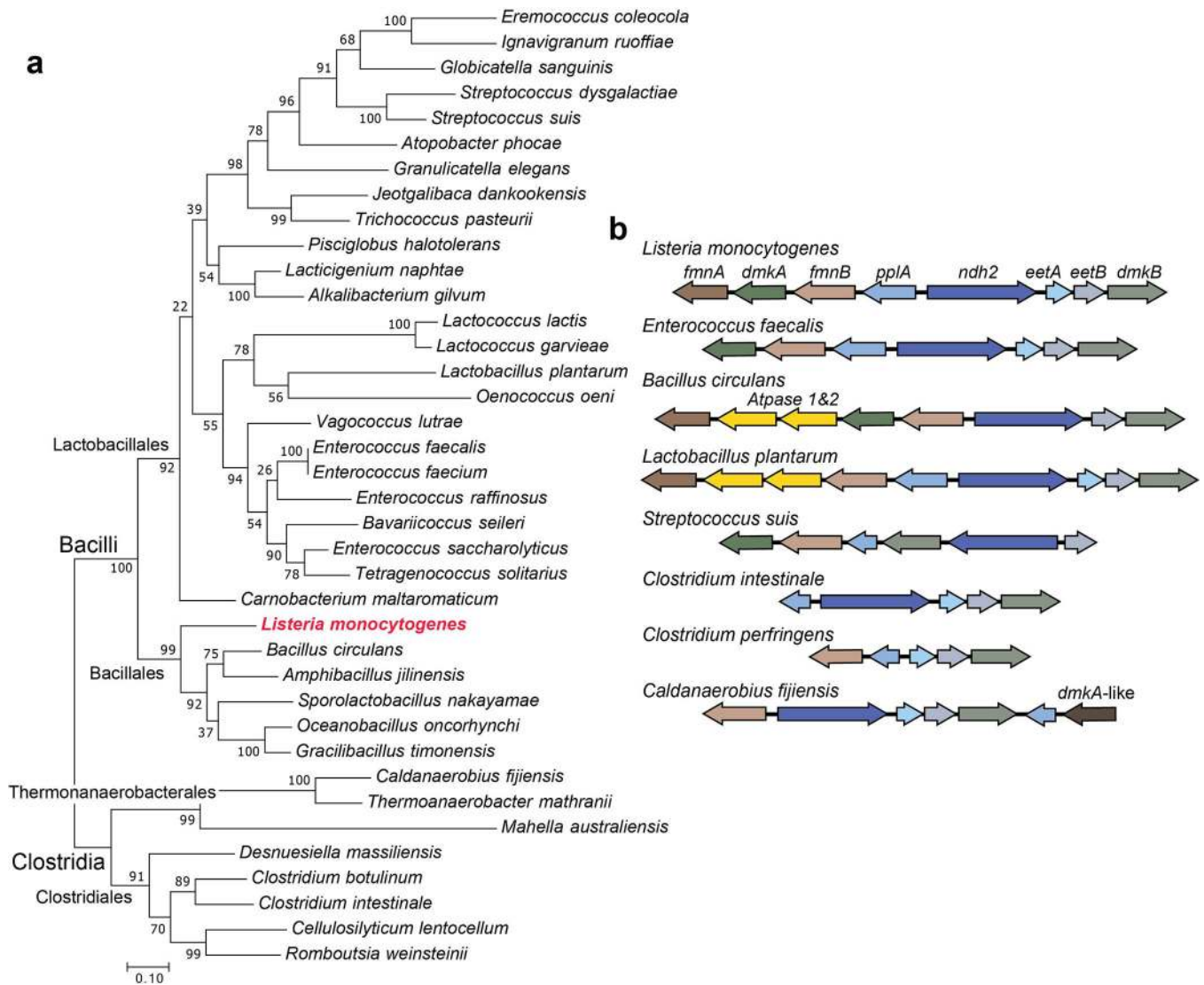
Extended Data Figure 9. Identified EET loci are widespread in the Firmicutes phylum.
(a) Phylogenetic tree constructed from select Ndh2 homolog sequences. A more comprehensive list of organisms that possess an EET locus is provided in Supplementary Table 3. The percentage of replicate trees that gave the depicted branch topology in a bootstrap test of 1,000 replicates is labeled. (b) Distinct EET loci from select genomes are shown. While the arrangement of genes varies, a locus with EET genes is present in many genomes. Some loci contain ECF transporter ATPase subunits (homologous to those depicted in Extended Data Fig. 5a) that likely function with RibU and FmnA subunits in flavin transport. The *dmkA*-like gene found in *Caldanaerobius fijiensis* (and other genomes) lacks homology to *dmkA*, but is annotated as catalyzing the same reaction. The *pplA* variant in some genomes contains a single FMNylated domain (rather than two) and this property is indicated by a shorter arrow. A few bacteria (including the *Lactococci*) lack a recognizable locus and distribute EET genes throughout the genome.

Supplementary Material

Refer to Web version on PubMed Central for supplementary material.

Acknowledgments

References

1. Shi L et al. Extracellular electron transfer mechanisms between microorganisms and minerals. Nat Rev Microbiol 14, 651–662, doi:10.1038/nrmicro.2016.93 (2016). [PubMed: 27573579]

2. Myers CR & Nealson KH Bacterial manganese reduction and growth with manganese oxide as the sole electron acceptor. Science 240, 1319–1321, doi:10.1126/science.240.4857.1319 (1988). [PubMed: 17815852]

3. Lovley DR & Phillips EJ Novel mode of microbial energy metabolism: organic carbon oxidation coupled to dissimilatory reduction of iron or manganese. Appl Environ Microbiol 54, 1472–1480 (1988). [PubMed: 16347658]

4. Carlson HK et al. Surface multiheme c-type cytochromes from *Thermincola potens* and implications for respiratory metal reduction by Gram-positive bacteria. Proc Natl Acad Sci U S A 109, 1702–1707, doi:10.1073/pnas.1112905109 (2012). [PubMed: 22307634]

5. Freitag NE, Port GC & Miner MD *Listeria monocytogenes* - from saprophyte to intracellular pathogen. Nat Rev Microbiol 7, 623–628, doi:10.1038/nrmicro2171 (2009). [PubMed: 19648949]

6. Deneer HG & Boychuk I Reduction of ferric iron by *Listeria monocytogenes* and other species of Listeria. Can J Microbiol 39, 480–485 (1993). [PubMed: 8330259]

7. Kim BH, Kim HJ, Hyun MS & Park DH Direct electrode reaction of Fe (III) reducing bacterium, Shewanella putrefacien*s*. Journal of microbiology and Biotechnology 9, 127–131 (1999).

8. Marsili E, Rollefson JB, Baron DB, Hozalski RM & Bond DR Microbial biofilm voltammetry: direct electrochemical characterization of catalytic electrode-attached biofilms. Appl Environ Microbiol 74, 7329–7337, doi:10.1128/AEM.00177-08 (2008). [PubMed: 18849456]

9. Xu S, El-Naggar M.Y JY. Disentangling the roles of free and cytochrome-bound flavins in extracellular electron transport from *Shewanella oneidensis* MR-1. Electrochimica Acta, 49–55, doi:10.1016/j.electacta.2016.03.074 (2016).

10. Karpowich NK, Song JM, Cocco N & Wang DN ATP binding drives substrate capture in an ECF transporter by a release-and-catch mechanism. Nat Struct Mol Biol 22, 565–571, doi:10.1038/nsmb.3040 (2015). [PubMed: 26052893]

11. Kerscher S, Drose S, Zickermann V & Brandt U The three families of respiratory NADH dehydrogenases. Results Probl Cell Differ 45, 185–222, doi:10.1007/400_2007_028 (2008). [PubMed: 17514372]

12. Unden G & Bongaerts J Alternative respiratory pathways of *Escherichia coli*: energetics and transcriptional regulation in response to electron acceptors. Biochim Biophys Acta 1320, 217–234 (1997). [PubMed: 9230919]

13. Bertsova YV et al. Alternative pyrimidine biosynthesis protein ApbE is a flavin transferase catalyzing covalent attachment of FMN to a threonine residue in bacterial flavoproteins. J Biol Chem 288, 14276–14286, doi:10.1074/jbc.M113.455402 (2013). [PubMed: 23558683]

14. Deka RK, Brautigam CA, Liu WZ, Tomchick DR & Norgard MV Evidence for Posttranslational Protein Flavinylation in the Syphilis Spirochete Treponema pallidum: Structural and Biochemical

Insights from the Catalytic Core of a Periplasmic Flavin-Trafficking Protein. MBio 6, e00519–00515, doi:10.1128/mBio.00519-15 (2015). [PubMed: 25944861]

15. Zuckert WR Secretion of bacterial lipoproteins: through the cytoplasmic membrane, the periplasm and beyond. Biochim Biophys Acta 1843, 1509–1516, doi:10.1016/j.bbamcr.2014.04.022 (2014). [PubMed: 24780125]

16. Glasser NR, Saunders SH & Newman DK The Colorful World of Extracellular Electron Shuttles. Annu Rev Microbiol 71, 731–751, doi:10.1146/annurev-micro-090816-093913 (2017). [PubMed: 28731847]

17. Brutinel ED & Gralnick JA Shuttling happens: soluble flavin mediators of extracellular electron transfer in *Shewanella*. Appl Microbiol Biotechnol 93, 41–48, doi:10.1007/s00253-011-3653-0 (2012). [PubMed: 22072194]

18. Marsili E et al. *Shewanella* secretes flavins that mediate extracellular electron transfer. Proc Natl Acad Sci U S A 105, 3968–3973, doi:10.1073/pnas.0710525105 (2008). [PubMed: 18316736]

19. von Canstein H, Ogawa J, Shimizu S & Lloyd JR Secretion of flavins by *Shewanella* species and their role in extracellular electron transfer. Appl Environ Microbiol 74, 615–623, doi:10.1128/AEM.01387-07 (2008). [PubMed: 18065612]

20. Kotloski NJ & Gralnick JA Flavin electron shuttles dominate extracellular electron transfer by Shewanella oneidensis. MBio 4, doi:10.1128/mBio.00553-12 (2013).

21. Powers HJ Riboflavin (vitamin B-2) and health. Am J Clin Nutr 77, 1352–1360, doi:10.1093/ajcn/77.6.1352 (2003). [PubMed: 12791609]

22. Huhner J, Ingles-Prieto A, Neususs C, Lammerhofer M & Janovjak H Quantification of riboflavin, flavin mononucleotide, and flavin adenine dinucleotide in mammalian model cells by CE with LED-induced fluorescence detection. Electrophoresis 36, 518–525, doi:10.1002/elps.201400451 (2015). [PubMed: 25488801]

23. Winter SE et al. Gut inflammation provides a respiratory electron acceptor for *Salmonella*. Nature 467, 426–429, doi:10.1038/nature09415 (2010). [PubMed: 20864996]

24. Winter SE et al. Host-derived nitrate boosts growth of *E. coli* in the inflamed gut. Science 339, 708–711, doi:10.1126/science.1232467 (2013). [PubMed: 23393266]

25. Slobodkin AI et al. Dissimilatory reduction of Fe(III) by thermophilic bacteria and archaea in deep subsurface petroleum reservoirs of western siberia. Curr Microbiol 39, 99–102 (1999). [PubMed: 10398835]

26. Roh Y et al. Isolation and characterization of metal-reducing thermoanaerobacter strains from deep subsurface environments of the Piceance Basin, Colorado. Appl Environ Microbiol 68, 6013–6020 (2002). [PubMed: 12450823]

27. Ogg CD & Patel BK *Fervidicola ferrireducens* gen. nov., sp. nov., a thermophilic anaerobic bacterium from geothermal waters of the Great Artesian Basin, Australia. Int J Syst Evol Microbiol 59, 1100–1107, doi:10.1099/ijs.0.004200-0 (2009). [PubMed: 19406800]

28. Ogg CD & Patel BK *Thermotalea metallivorans* gen. nov., sp. nov., a thermophilic, anaerobic bacterium from the Great Artesian Basin of Australia aquifer. Int J Syst Evol Microbiol 59, 964–971, doi:10.1099/ijs.0.004218-0 (2009). [PubMed: 19406776]

29. Ogg CD, Greene AC & Patel BK Thermovenabulum gondwanense sp. nov., a thermophilic anaerobic Fe(III)-reducing bacterium isolated from microbial mats thriving in a Great Artesian Basin bore runoff channel. Int J Syst Evol Microbiol 60, 1079–1084, doi:10.1099/ijs.0.009886-0 (2010). [PubMed: 19666811]

30. Ogg CD & Patel BK *Fervidicella metallireducens* gen. nov., sp. nov., a thermophilic, anaerobic bacterium from geothermal waters. Int J Syst Evol Microbiol 60, 1394–1400, doi:10.1099/ijs.0.014670-0 (2010). [PubMed: 19671710]

31. Masuda M, Freguia S, Wang YF, Tsujimura S & Kano K Flavins contained in yeast extract are exploited for anodic electron transfer by *Lactococcus lactis*. Bioelectrochemistry 78, 173–175, doi:10.1016/j.bioelechem.2009.08.004 (2010). [PubMed: 19717350]

32. Zhang E, Cai Y, Luo Y & Piao Z Riboflavin-shuttled extracellular electron transfer from *Enterococcus faecalis* to electrodes in microbial fuel cells. Can J Microbiol 60, 753–759, doi:10.1139/cjm-2014-0389 (2014). [PubMed: 25345758]

33. Dong Y et al. *Orenia metallireducens* sp. nov. Strain Z6, a Novel Metal-Reducing Member of the Phylum Firmicutes from the Deep Subsurface. Appl Environ Microbiol 82, 6440–6453, doi: 10.1128/AEM.02382-16 (2016). [PubMed: 27565620]

34. Keogh D et al. Extracellular Electron Transfer Powers Enterococcus faecalis Biofilm Metabolism. MBio 9, doi:10.1128/mBio.00626-17 (2018).

35. Pankratova G, Leech D, Gorton L & Hederstedt L Extracellular Electron Transfer by the Gram-Positive Bacterium *Enterococcus faecalis*. Biochemistry, doi:10.1021/acs.biochem.8b00600 (2018).

36. Pedersen MB, Gaudu P, Lechardeur D, Petit MA & Gruss A Aerobic respiration metabolism in lactic acid bacteria and uses in biotechnology. Annu Rev Food Sci Technol 3, 37–58, doi:10.1146/annurev-food-022811-101255 (2012). [PubMed: 22385163]

37. Hodgson DA Generalized transduction of serotype 1/2 and serotype 4b strains of *Listeria monocytogenes*. Mol Microbiol 35, 312–323 (2000). [PubMed: 10652092]

38. Zemansky J et al. Development of a mariner-based transposon and identification of *Listeria monocytogenes* determinants, including the peptidyl-prolyl isomerase PrsA2, that contribute to its hemolytic phenotype. J Bacteriol 191, 3950–3964, doi:10.1128/JB.00016-09 (2009). [PubMed: 19376879]

39. Whiteley AT, Pollock AJ & Portnoy DA The PAMP c-di-AMP Is Essential for Listeria monocytogenes Growth in Rich but Not Minimal Media due to a Toxic Increase in (p)ppGpp. [corrected]. Cell Host Microbe 17, 788–798, doi:10.1016/j.chom.2015.05.006 (2015). [PubMed: 26028365]

40. Xayarath B, Alonzo F, 3rd & Freitag NE Identification of a peptide-pheromone that enhances *Listeria monocytogenes* escape from host cell vacuoles. PLoS Pathog 11, e1004707, doi:10.1371/journal.ppat.1004707 (2015). [PubMed: 25822753]

41. Burke TP et al. *Listeria monocytogenes* is resistant to lysozyme through the regulation, not the acquisition, of cell wall-modifying enzymes. J Bacteriol 196, 3756–3767, doi:10.1128/JB.02053-14 (2014). [PubMed: 25157076]

42. Lovley DR & Phillips EJ Organic matter mineralization with reduction of ferric iron in anaerobic sediments. Appl Environ Microbiol 51, 683–689 (1986). [PubMed: 16347032]

43. Light SH, Cahoon LA, Halavaty AS, Freitag NE & Anderson WF Structure to function of an alpha-glucan metabolic pathway that promotes *Listeria monocytogenes* pathogenesis. Nat Microbiol 2, 16202, doi:10.1038/nmicrobiol.2016.202 (2016). [PubMed: 27819654]

44. Portnoy DA, Jacks PS & Hinrichs DJ Role of hemolysin for the intracellular growth of *Listeria monocytogenes*. J Exp Med 167, 1459–1471 (1988). [PubMed: 2833557]

45. Bou Ghanem EN et al. InlA promotes dissemination of Listeria monocytogenes to the mesenteric lymph nodes during food borne infection of mice. PLoS Pathog 8, e1003015, doi:10.1371/journal.ppat.1003015 (2012). [PubMed: 23166492]

46. Becattini S et al. Commensal microbes provide first line defense against *Listeria monocytogenes* infection. J Exp Med 214, 1973–1989, doi:10.1084/jem.20170495 (2017). [PubMed: 28588016]

47. Auerbuch V, Lenz LL & Portnoy DA Development of a competitive index assay to evaluate the virulence of *Listeria monocytogenes* actA mutants during primary and secondary infection of mice. Infect Immun 69, 5953–5957 (2001). [PubMed: 11500481]

48. Neilson KA et al. Less label, more free: approaches in label-free quantitative mass spectrometry. Proteomics 11, 535–553, doi:10.1002/pmic.201000553 (2011). [PubMed: 21243637]

49. Nahnsen S, Bielow C, Reinert K & Kohlbacher O Tools for label-free peptide quantification. Mol Cell Proteomics 12, 549–556, doi:10.1074/mcp.R112.025163 (2013). [PubMed: 23250051]

50. Plumb RS et al. UPLC/MS(E); a new approach for generating molecular fragment information for biomarker structure elucidation. Rapid Commun Mass Spectrom 20, 1989–1994, doi:10.1002/rcm.2550 (2006). [PubMed: 16755610]

51. Shliaha PV, Bond NJ, Gatto L & Lilley KS Effects of traveling wave ion mobility separation on data independent acquisition in proteomics studies. J Proteome Res 12, 2323–2339, doi:10.1021/pr300775k (2013). [PubMed: 23514362]

52. Altschul SF et al. Gapped BLAST and PSI-BLAST: a new generation of protein database search programs. Nucleic Acids Res 25, 3389–3402 (1997). [PubMed: 9254694]

53. Larkin MA et al. Clustal W and Clustal X version 2.0. Bioinformatics 23, 2947–2948, doi:10.1093/ bioinformatics/btm404 (2007). [PubMed: 17846036]

54. Jones DT, Taylor WR & Thornton JM The rapid generation of mutation data matrices from protein sequences. Comput Appl Biosci 8, 275–282 (1992). [PubMed: 1633570]

55. Kumar S, Stecher G & Tamura K MEGA7: Molecular Evolutionary Genetics Analysis Version 7.0 for Bigger Datasets. Mol Biol Evol 33, 1870–1874, doi:10.1093/molbev/msw054 (2016). [PubMed: 27004904]

56. Becavin C et al. Comparison of widely used Listeria monocytogenes strains EGD, 10403S, and EGD-e highlights genomic variations underlying differences in pathogenicity. MBio 5, e00969–00914, doi:10.1128/mBio.00969-14 (2014). [PubMed: 24667708]

57. Jones S & Portnoy DA Characterization of *Listeria monocytogenes* pathogenesis in a strain expressing perfringolysin O in place of listeriolysin O. Infect Immun 62, 5608–5613 (1994). [PubMed: 7960143]

58. Chen GY, McDougal CE, D'Antonio MA, Portman JL & Sauer JD A Genetic Screen Reveals that Synthesis of 1,4-Dihydroxy-2-Naphthoate (DHNA), but Not Full-Length Menaquinone, Is Required for Listeria monocytogenes Cytosolic Survival. MBio 8, doi:10.1128/mBio.00119-17 (2017).
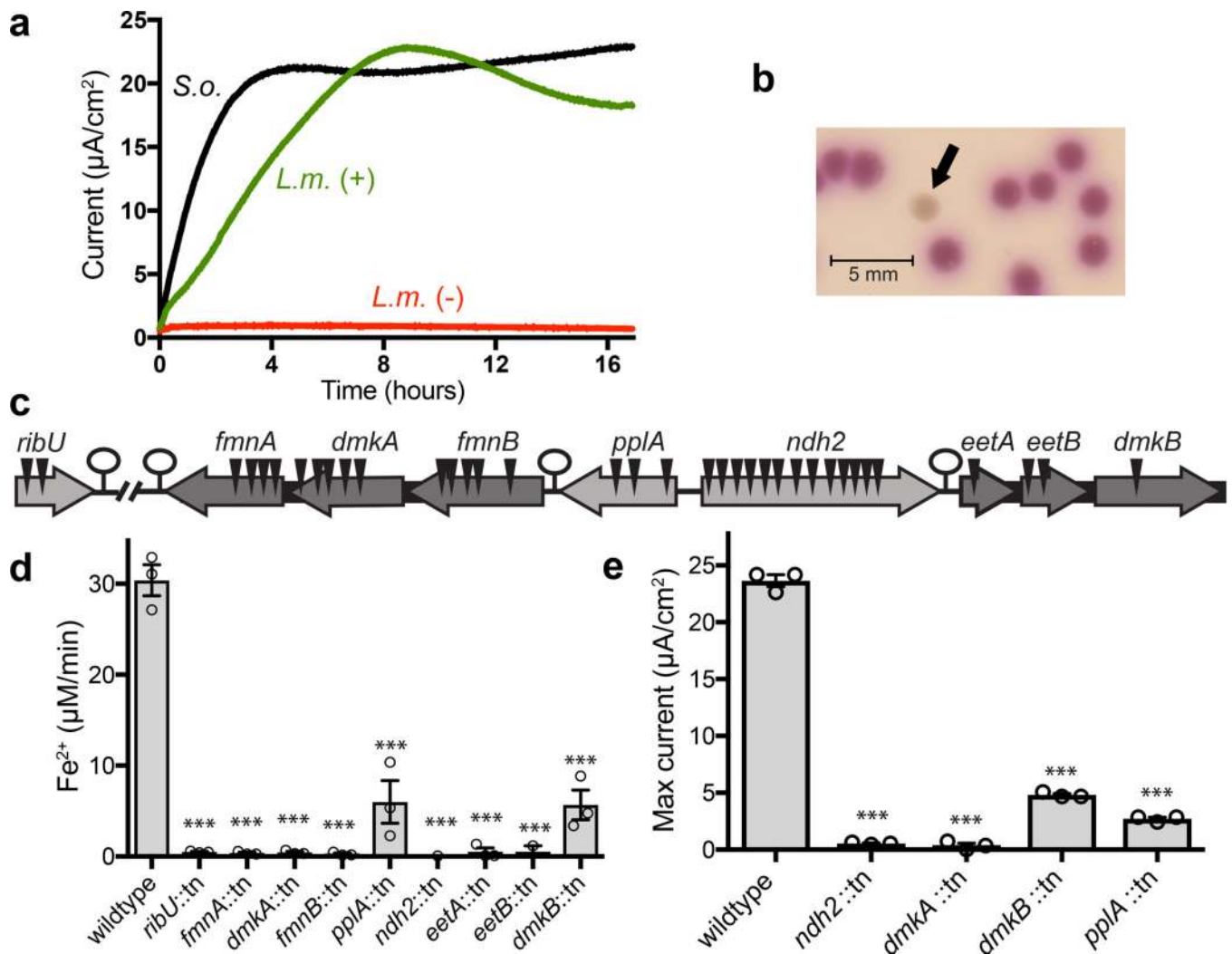
Fig. 1. An uncharacterized genetic locus associated with EET activity.
(a) Chronoamperometry results from *L. monocytogenes (L.m.) or Shewanella oneidensis (S.o.)*-inoculated electrochemical reactors. For *L. monocytogenes* experiments, the +/− signify whether electron donor (glucose) was included in the medium; lactate was used as an electron donor for *S. oneidensis*. Results are representative of three independent experiments (*n* = 3). (b) A representative of the thirty-six independent mutants identified from the ferric iron reduction screen minutes after ferrozine agar overlay (arrow). (c) Location of transposon insertions (triangles) in mutants identified as having decreased ferric iron reductase activity in the genetic screen. Arrows represent genes, with the darker gray signifying inclusion in a multi-gene operon. Previously uncharacterized genes on the locus have been assigned names based on putative functions. (d) Ferric iron reductase activity of transposon mutants identified from the screen. Results are expressed as means and standard errors from three independent experiments (*n* = 3). (e) Maximum electric current achieved from chronoamperometry experiments with representative EET mutants. Strains that statistically differ from wildtype (***, *P* < 0.001 [ANOVA with Dunnett's posttest]) are indicated.
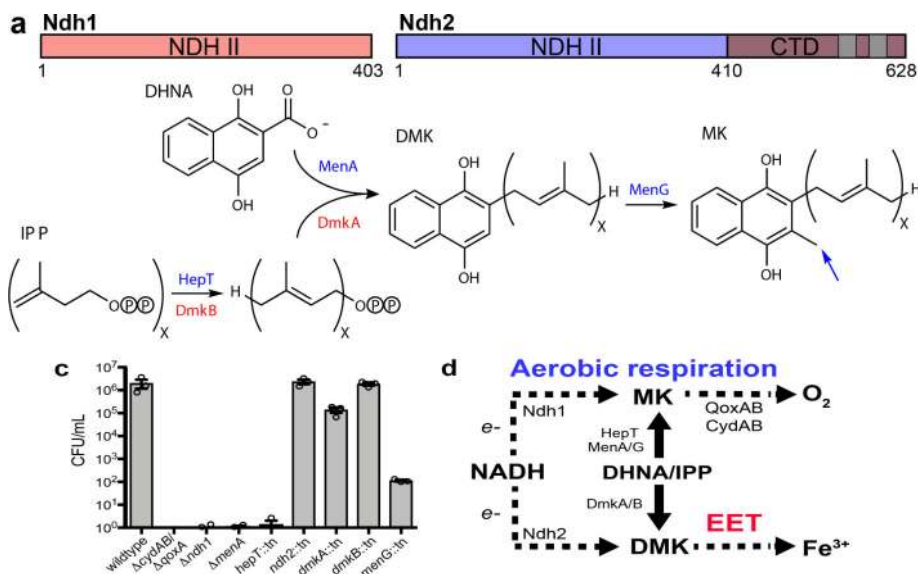
Fig. 2. A parallel electron transfer pathway segregates EET from aerobic respiration.
(a) Domain layout of *L. monocytogenes* proteins Ndh1 and Ndh2. Abbreviations stand for type II NADH dehydrogenase domain (NDH II) and C-terminal domain (CTD). Gray regions represent predicted transmembrane helices. (b) Predicted reactions catalyzed by DmkA/DmkB and paralogous *L. monocytogenes* proteins MenA/HepT, as well as MenG (highlighted by blue arrow). Abbreviations stand for demethylmenaquinone (DMK), menaquinone (MK), isopentenyl pyrophosphate (IPP), and 1,4-dihydroxy-2-napthoyl-CoA (DHNA). The 'x' refers to an unknown number of isoprene repeats, which may differ between the two quinones. (c) Colony-forming units (CFU) after 24 hours in "aerobic respiration medium." Results ($n = 3$) are expressed as means and standard errors. The $\Delta cydAB/\Delta qoxA$ mutant lacks terminal cytochrome oxidases and thus provides an aerobic respiration-deficient control. (d) Probable electron transfer pathways inferred from mutants with EET (red) or aerobic respiration (blue) phenotypes. Dashed arrows highlight the path of electron flow and solid lines track quinone synthesis.
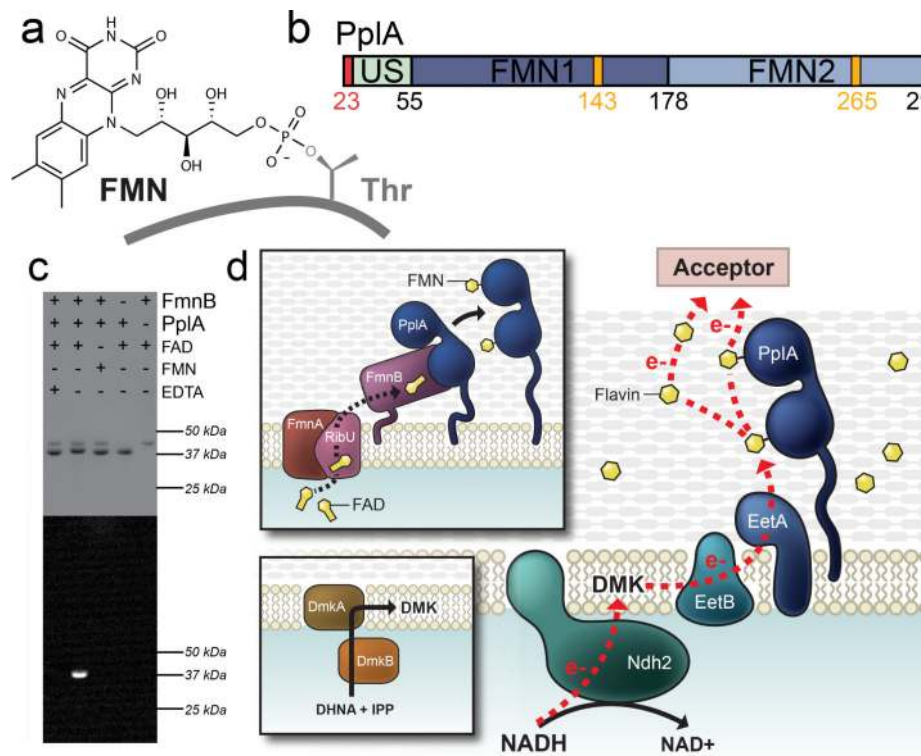
Fig. 3. A surface-associated flavoprotein establishes the extracellular component of EET apparatus.

(a) Post-translational modification catalyzed by the FMN transferase family of enzymes, of which FmnB is a member.[13,14] (b) Domain architecture of PplA. Abbreviations stand for: unstructured (US), FMNylated domain 1 (FMN1), and FMNylated domain 2 (FMN2). The lipidated cysteine on the N-terminus after signal peptidase processing is colored red and FMNylated threonines yellow. (c) Analysis of FmnB substrate specificity. SDS-PAGE of recombinant PplA after incubation under specified conditions. UV illumination of the gel (bottom) allows for visualization of protein with covalently bound flavin. Results are representative of three independent experiments ($n = 3$). See Supplementary Figure 1 for uncropped gel. (d) Model of the molecular basis of EET. DmkA and DmkB synthesize a demethylmenaquinone (DMK) derivative (lower inset). RibU and FmnA secrete FAD that is used by FmnB to post-translationally modify PplA (upper inset). EET is achieved by a series of electron transfers. Ndh2 transfers electrons from NAD to DMK. Electrons are transferred from DMK to FMN groups on PplA or free flavin shuttles – possibly with involvement from uncharacterized membrane proteins in the EET locus, EetA and EetB – and ultimately to terminal electron acceptor.
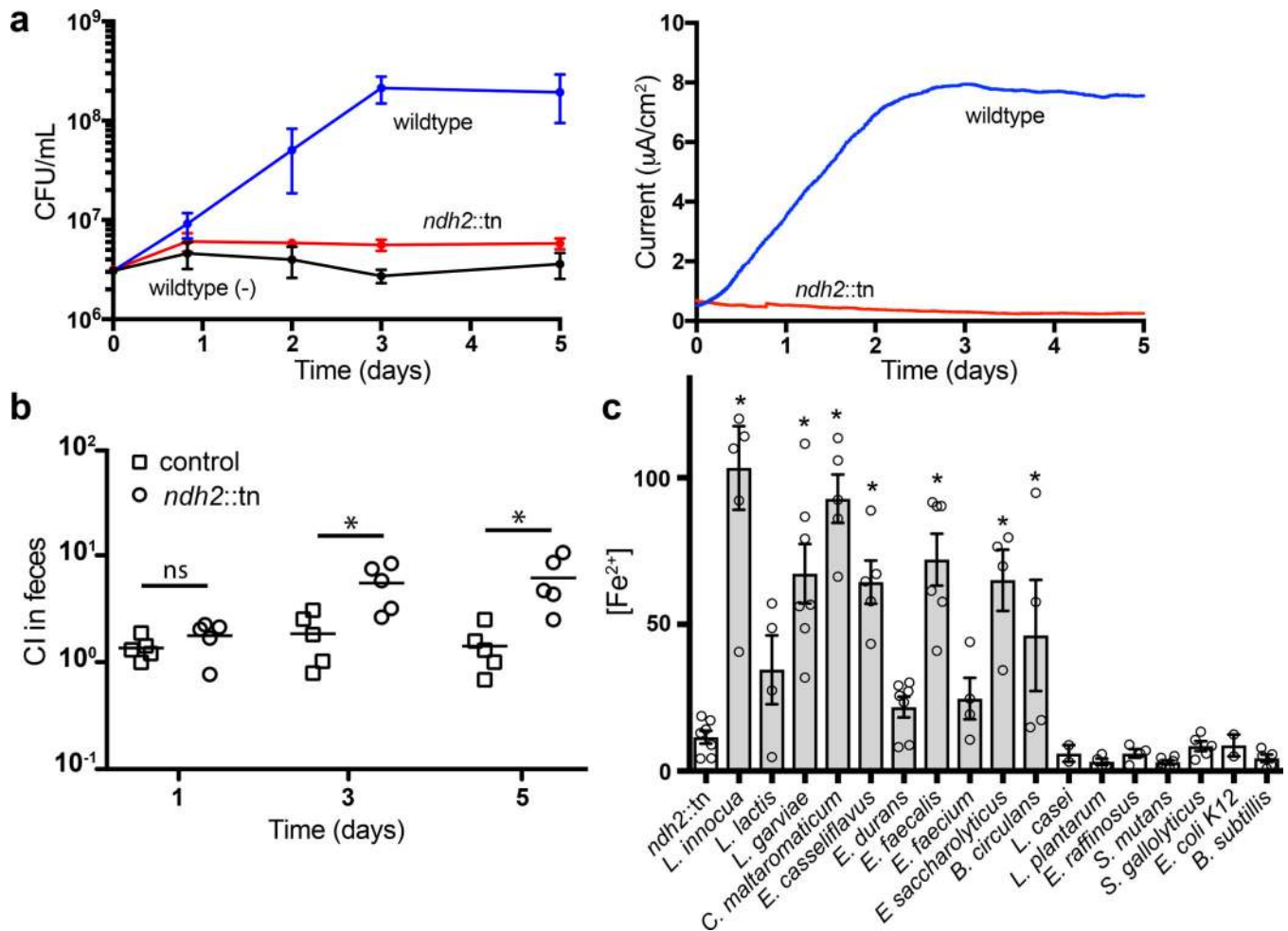
Fig. 4. EET supports anaerobic growth, confers a competitive advantage in the intestinal lumen, and is active in multiple Firmicutes.

(a) *L. monocytogenes* CFU (left) and electric current (right) from chronoamperometry experiments conducted with xylitol growth medium. The (−) signifies a control condition without an electrode. Results from three independent experiments (*n* = 3) are expressed as means and standard errors. (b) Mice (*n* = 5) were fed bread inoculated with a 1:1 mixture of Δ*hly L. monocytogenes* and Δ*hly/ndh2*::tn strains. The competitive index at three post-infection time points is indicated. Median values and statistically significant differences (*, *P* = 0.01 [unpaired two-sided *t* test]) between the Δ*hly/ndh2*::tn mutant and a control that competed two Δ*hly* strains are indicated. Results are representative of three independent experiments (*n* = 3). (c) Iron reductase activity in a panel of Firmicutes species, expressed as a percentage of wildtype *L. monocytogenes* activity. Results from at least three independent experiments (*n* = 7 for *ndh2*::tn, *L. garviae*, *E. durans*; *n* = 6 for *L. innocua E. faecalis S. mutans*; *n* = 5 for *C. maltaromaticum, E. casseliflavus, S. gallolyticus, B. subtillis*; *n* = 4 for *L. lactis, E. faecium, E saccharolyticus, B. circulans, L. plantarum, E. raffinosus*; *n* = 3 for *L. casei, E. coli* K12) are expressed in arbitrary units as means and standard errors. Strains that statistically differ from *ndh2*::tn are indicated (*, *P* < 0.05 [ANOVA with Dunnett's posttest]). Some Lactobacillales lack the ability to synthesize 1,4-dihydroxy-2-napthoyl-

CoA (DHNA), the precursor for demethylmenaquinone biosynthesis, and require an exogenous source for quinone-dependent processes.[36] Organisms with EET genes and *menC* (which catalyzes an essential step in DHNA biosynthesis) are colored gray. *L. casei*, *L. plantarum* and *E. raffinosus* contain genes for EET, but not *menC*. The remaining species lack EET genes.